Supplementary Materials - Noninvasive Electromagnetic Source Imaging and Granger Causality Analysis: An Electrophysiological Connectome (eConnectome) Approach

Abbas Sohrabpour, *Student Member, IEEE*, Shuai Ye, Gregory A. Worrell, Wenbo Zhang, and Bin He*, *Fellow, IEEE; binhe@umn.edu*

I. Some Details About the Multivariate Autoregressive (MVAR) Model Implementation

The coefficients of the MVAR model were computed using a Kalman filter algorithm through a recursive least squares (RLS) implementation with forgetting factors [1]–[3]. The model order, P, was selected based on Akaike Information Criterion (AIC). The model orders estimated with AIC were very close to the model orders used for the simulation studies. All implementations were based on eConnectome software (open source software available freely at http://econnectome.umn.edu). Please refer to eConnectome manual for more information.

II. Some Details About the Noise Model

There are three sources of noise in our simulations in this study. One is the innovations that drive the autoregressive model (considered as part of the signal), white uncorrelated noise added to the simulated EEG data (at sensor space) and the white noise added to all dipole locations in the source space (modeling background noise activity which represents as correlated noise in the sensor space). The signal-to-noise ratios (SNR) reported in this study are the mean SNR calculated as the mean power of the EEG signals from simulated underlying sources over the mean power of noise from additive white noise in the sensor space and background noise whenever present (remember that two models were used in this paper, one where no correlated noise was added which are presented in the main body and one with correlated noise presented in the following). The underlying sources are generated based on an MVAR model and thus include the uncorrelated noise, or innovations, which is treated as part of the desirable signal and hence calculated as power of the signal and not noise. SNR was reported in log-scale and hence reported as dB throughout the work.

III. The Effect of Correlated Noise

In order to more realistically model the problem, a new set of simulations studies were conducted in which correlated noise (in sensor space) was also included (in addition to the white noise added in sensor level modeling the measurement noise). White Gaussian noise was added in all source locations to model background activity of the brain [4], thus source level and sensor level noise were included in this new simulation study to better model various possible noise sources. The reported SNR is the total SNR due to sensor and source space noise. The results of these simulations are presented in the supplementary section

(Fig. S1). The results (in terms of localization error of network nodes and connectivity measures) do not change drastically. Additionally to compare the results more easily to our original simulation, we have placed the results from the original simulation in the same order as Fig. S1 in Fig. C1 (both figures follow). Comparing Fig. C1 and Fig. S1, it can be seen that not much difference is observed, and the proposed technique can still delineate underlying networks from noninvasive EEG recordings.

IV. Sensitivity and Specificity of DTF and PDC in Determining The Underlying Connectivity of Brain Networks

In order to more intuitively comprehend the performance of DTF and PDC in determining the underlying connectivity of brain networks, we calculate and report the value of sensitivity and specificity of each method in detecting network links. The results are presented in Table S0 in the following and correspond to the data presented in Fig. 5 and Fig. 6 in the main body. Sensitivity is defined as the ratio of true positives (detected links where a link is expected, i.e. simulated) over the positives (number of all existing links) and indicates the ability of each method in retrieving existing links. Specificity is defined as the ratio of true negatives (not detecting links where a link is not expected, i.e. no links simulated) over the negatives (number of nullities where no link exists, i.e. simulated) and intuitively shows how well the detection of false links can be avoided by the specific method.

Looking at the results presented in Tables I-IV, it can be observed that both methods have high specificity and sensitivity, which is desirable. However, PDC seems to have higher specificity compared to DTF while both have very similar sensitivity. This is expected as discussed in the main body. PDC is shown to retrieve direct links while DTF detects direct and indirect links. This means that while both will have high sensitivity values (meaning both detect the existing links very well), but PDC will have slightly higher specificity (meaning that it better rejects indirect links which might be detected by DTF).

TABLE I
SENSITIVITY FOR DTF METHOD

		Number of Electrodes			
		32	*64*	*128*	*256*
SNR (dB)	***5 dB***	**0.71**	**0.63**	**0.68**	**0.7**
	10dB	**0.69**	**0.71**	**0.86**	**0.84**
	20dB	**0.86**	**0.82**	**0.87**	**0.83**

Sensitivity of the DTF in determining the underlying links of the brain networks for various SNR levels and electrode configurations.

TABLE II
SENSITIVITY FOR PDC METHOD

		Number of Electrodes			
		32	*64*	*128*	*256*
SNR (dB)	***5 dB***	**0.59**	**0.6**	**0.62**	**0.77**
	10dB	**0.52**	**0.58**	**0.86**	**0.81**
	20dB	**0.78**	**0.84**	**0.89**	**0.92**

Sensitivity of the PDC in determining the underlying links of the brain networks for various SNR levels and electrode configurations.

TABLE III
SPECIFICITY FOR DTF METHOD

		Number of Electrodes			
		32	*64*	*128*	*256*
SNR (dB)	***5 dB***	**0.42**	**0.59**	**0.52**	**0.61**
	10dB	**0.49**	**0.51**	**0.59**	**0.51**
	20dB	**0.38**	**0.54**	**0.67**	**0.72**

Specificity of the DTF in determining the underlying links of the brain networks for various SNR levels and electrode configurations.

TABLE IV
SPECIFICITY FOR PDC METHOD

		Number of Electrodes			
		32	*64*	*128*	*256*
SNR (dB)	***5 dB***	**0.73**	**0.64**	**0.62**	**0.73**
	10dB	**0.67**	**0.67**	**0.8**	**0.8**
	20dB	**0.54**	**0.83**	**0.93**	**0.96**

Specificity of the PDC in determining the underlying links of the brain networks for various SNR levels and electrode configurations.

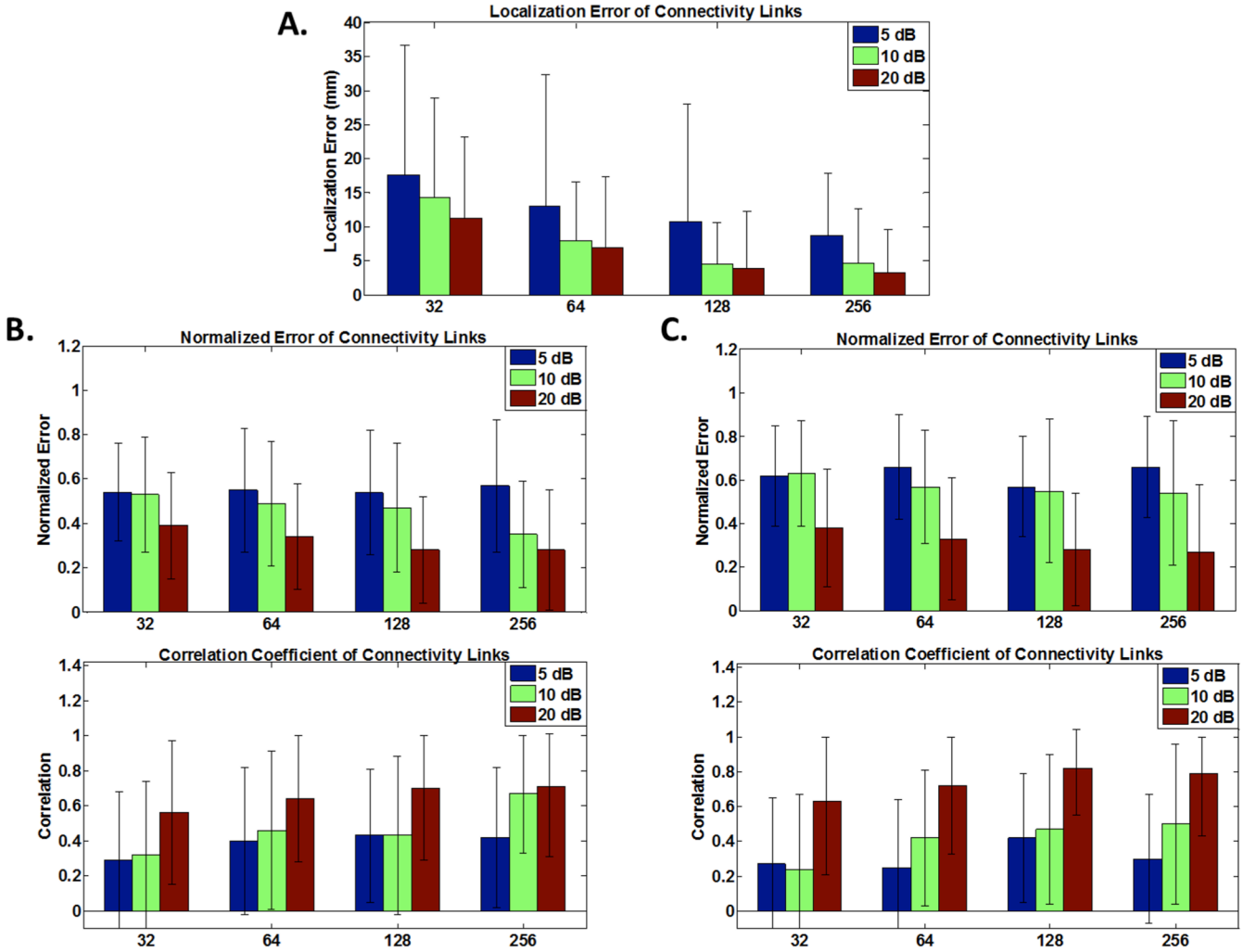

Fig. S1. Simulation results for correlated noise. The localization error of network nodes (A), connectivity metrics for DTF analysis (B) and PDC analysis (C) are presented for the Monte Carlo simulations. Normalized error (middle row) and correlation (bottom row) are used to assess the performance of the proposed method. Compare results to Fig. C1. Error bars depict standard deviation.

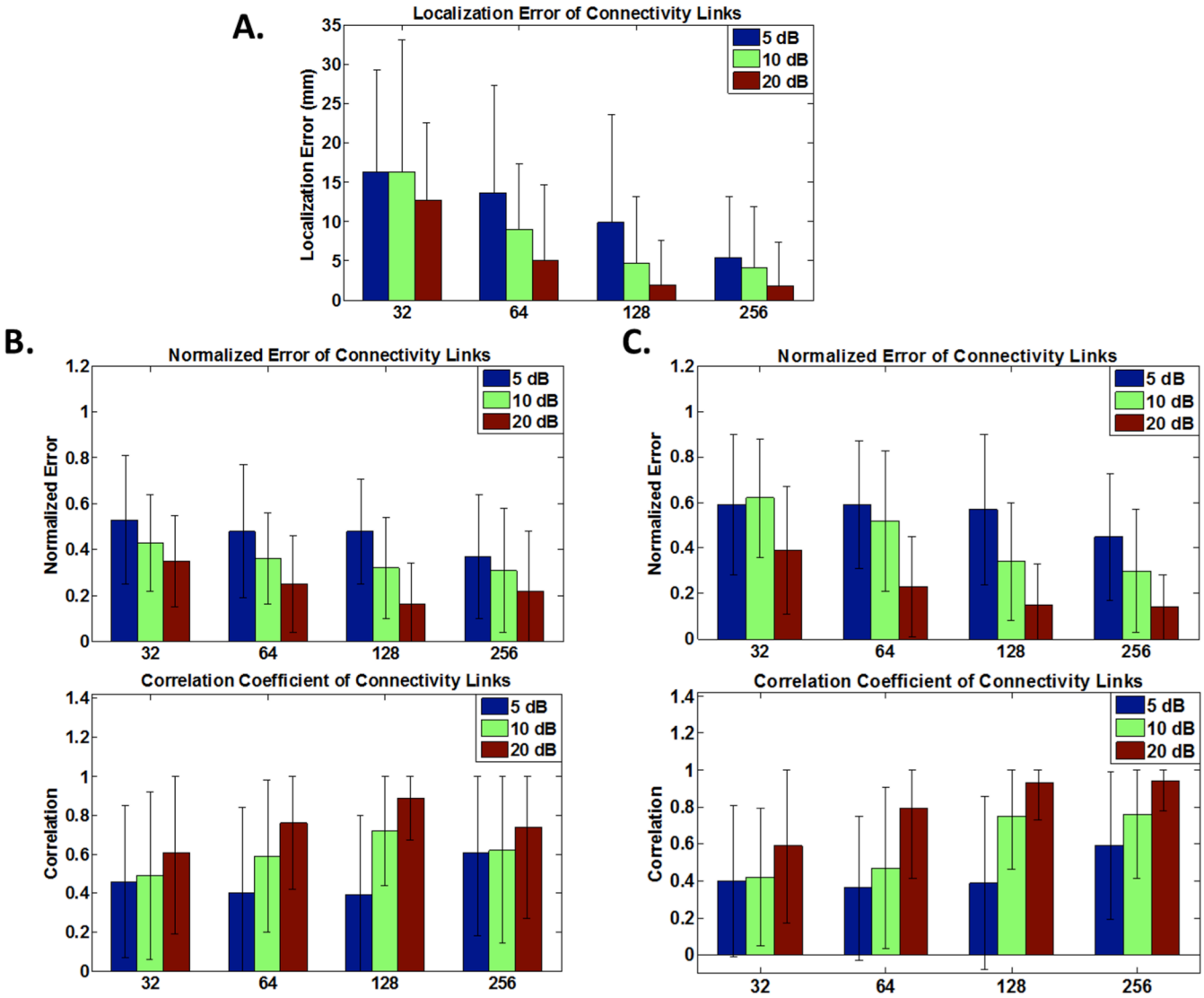

Fig. C1. Simulation results for white noise (original results re-arranged). The localization error of network nodes (A), connectivity metrics for DTF analysis (B) and PDC analysis (C) are presented for the Monte Carlo simulations. Normalized error (middle row) and correlation (bottom row) are used to assess the performance of the proposed method. Compare results to Fig. S1. Error bars depict standard deviation.

REFERENCES

[1] M. Arnold *et al.*, "Adaptive AR modeling of nonstationary time series by means of Kalman filtering," *IEEE Transactions on Biomedical Engineering*, vol. 45, no. 5, pp. 553–562, 1998.

[2] M. Campi, "Performance of RLS identification algorithms with forgetting factor: A φ-mixing approach," in *J. Math. Systems Estim. Control*, 1994.

[3] H. Akaike, "A new look at the statistical model identification," *Automatic Control, IEEE Transactions on*, vol. 19, no. 6, pp. 716–723, 1974.

[4] F. Babiloni *et al.*, "Multimodal integration of EEG and MEG data: A simulation study with variable signal-to-noise ratio and number of sensors," *Human brain mapping*, vol. 22, no. 1, pp. 52–62, 2004.